

Partially Fluorinated Maleimide Copolymers for Langmuir Films of Improved Stability. 2. Spreading Behavior and Multilayer Formation

Peter Hendlinger,^{†,‡} André Laschewsky,^{*,†} Patrick Bertrand,[§] Arnaud Delcorte,[§] Roger Legras,[§] Bernard Nysten,[§] and Dietmar Möbius^{||}

Departments of Chemistry and Material Science, Université Catholique de Louvain, Place L. Pasteur 1, B-1348 Louvain-la-Neuve, Belgium, and MPI Biophysikalische Chemie, Göttingen, Germany

Received June 26, 1996. In Final Form: October 22, 1996[⊗]

The spreading behavior and multilayer formation of partially fluorinated alternating copolymers are studied. The copolymers are based on substituted *N*-phenylmaleimides which lack standard hydrophilic groups as well as aliphatic hydrophobic chains. The stability of such vinyl copolymers against thermal degradation is exceptionally high, as are their glass transition temperatures. Despite their unconventional structure, the copolymers form stable monolayers with high collapse pressures. The surface potential of monolayers can be adjusted between positive and negative potentials by well-placed fluorinated substituents. Also, multilayers can be built up by the Langmuir–Blodgett technique.

Introduction

Generally, Langmuir–Blodgett (LB) films are very sensitive to thermal and mechanical stress. Though the use of polymers has considerably reduced this sensitivity,¹ classical polymeric LB films still suffer from limited chemical and mechanical stability,^{2,3} confining proposed applications generally to temperatures below 150 °C.⁴ This is partially due to the use of standard amphiphilic side groups which are pyrolytically sensitive, as well as of polymer backbones with limited thermal stability, as in the case of the most widely used poly(meth)acrylics which begin to decompose at 200 °C. Additionally, the long hydrocarbon chains present lead to low melting temperatures and to low glass transition temperatures T_g , respectively.

More stable polymeric systems have been occasionally studied such as polyimides,^{5,6} polybenzimidazoles,⁷ polybenzothiazoles,⁶ or polymeric Schiff bases,⁸ but their synthesis is demanding and often incompatible with functionalization. Also, such polymers are generally poorly soluble, thus requiring the use of precursor polymers and subsequent curing within the LB films.

As alternative systems, we have recently synthesized new alternating copolymers based on substituted *N*-phenylmaleimides with various electron-rich comonomers such as styrenes and vinyl ethers.⁹ Conveniently prepared by free radical copolymerization, the alternating copoly-

mers are chemically well-defined in comparison to statistical copolymers. Though the spreading of some copolymers of maleimides with vinyl ethers has been reported in the past, the copolymers were always composed of a rather classical amphiphilic structure bearing hydrophobic alkyl chains, ranging from butyl to octadecyl chains.^{10,11} Here in contrast, the long aliphatic hydrophobic side chains are replaced by aryl groups which partially carry fluorinated substituents, to increase hydrophobicity (see Table 1). Moreover, standard hydrophilic but thermolabile groups are missing. The polar groups are confined exclusively to the inherently present imide moieties, which in some cases are supported by ether moieties. Both strategies were found to improve thermal and thermomechanical behavior considerably, resulting in onset temperatures for pyrolysis up to 400 °C and in glass transition temperatures up to 260 °C.⁹ Table 1 lists the copolymers investigated. For comparison, copolymer **11f** with a “classical” amphiphilic structure is studied, which is made from a hydrophilic maleimide with an electron-rich vinyl ether carrying a long hydrocarbon chain. As an intermediate case with respect to amphiphilic structure and thermal stability, copolymers **10a–d** made from *N*-phenylmaleimides with the hydrophilic comonomer *N*-vinylpyrrolidone⁹ are included, too.

The self-organization of macromolecules in well-defined monolayers requires the rearrangement of random, three-dimensional coils which are in general formed in bulk solution, into a two-dimensional conformation at the gas–water interface.¹ This is either due to the self-organization of amphiphilic side groups as observed for polymerized lipids.^{2,3,12,13} (In this case, the main chain must adjust appropriately to allow a monolayer packing of the amphiphilic side groups.) or, to the self-organization of the polymer backbone—with the side groups adjusting—as

* Author for correspondence.

[†] Department of Chemistry, Université Catholique de Louvain.

[‡] Permanent address: Universität Mainz, Institut Organische Chemie, D-55099 Mainz, Germany.

[§] Department of Material Science, Université Catholique de Louvain.

^{||} MPI Biophysikalische Chemie, D-37077 Göttingen.

[⊗] Abstract published in *Advance ACS Abstracts*, January 1, 1997.

(1) Gaines, G. L. *Langmuir* **1991**, *7*, 834.

(2) Embs, F.; Funhoff, D.; Laschewsky, A.; Licht, U.; Ohst, H.; Prass, W.; Ringsdorf, H.; Wegner, G.; Wehrmann, R. *Adv. Mater.* **1991**, *3*, 25.

(3) Shimomura, M. *Prog. Polym. Sci.* **1993**, *18*, 295.

(4) Erdelen, C.; Laschewsky, A.; Ringsdorf, H.; Schneider, J.; Schuster, A. *Thin Solid Films* **1989**, *180*, 153.

(5) Bliznyuk, V. N.; Ponomarev, I. I.; Rusanov, A. L. *Thin Solid Films* **1994**, *237*, 231.

(6) Kakimoto, M.; Imai, Y. *Macromol. Symp.* **1995**, *98*, 1123.

(7) Fowler, M. T.; Suzuki, M.; Engel, A. K.; Asano, K.; Itoh, T. *J. Appl. Phys.* **1987**, *62*, 3427.

(8) Engel, A. K.; Yoden, T.; Sanui, K.; Ogata, N. *J. Am. Chem. Soc.* **1985**, *107*, 8308.

(9) El-Guweri, M.; Hendlinger, P.; Laschewsky, A. *Macromol. Chem. Phys.*, in press.

(10) Anton, P.; Laschewsky, A. *Makromol. Chem.* **1993**, *194*, 601.

(11) Tebbe, H.; von Ackern, F.; Tieke, B. *Macromol. Chem. Phys.* **1995**, *196*, 1475.

(12) Elbert, R.; Laschewsky, A.; Ringsdorf, H. *J. Am. Chem. Soc.* **1985**, *107*, 4134.

(13) Laschewsky, A.; Ringsdorf, H.; Schmidt, G.; Schneider, J. *J. Am. Chem. Soc.* **1987**, *109*, 788.

Table 1. Structure of the Maleimide Copolymers Studied

		R ³ = -H					TYPE
R ²	R ¹						
		1a		1c		1e	V
		2a	2b	2c	2d		V
		3a		3c	3d		V
			4b				V
		5a				5e	V
				6c			V
		7a	7b	7c	7d		IV
		8a	8b	8c	8d	8e	VI
		9a	9b	9c	9d	9e	III
		10a	10b	10c	10d		II
						11f	I

observed for some polypeptides¹⁴ and "rigid rod" polymers.^{2,15–18} In any case, a minimal amphiphilic character is needed to allow successful spreading.^{17,18} If the polymer does not self-organize at the interface, a more or less deformed three-dimensional polymer coil is expected. Between these three extremes, i.e., self-organization of the side groups, self-organization of the backbone, or no spreading, any intermediate situation could be found, giving rise to partial monolayer formation. Only optimized polymers will come close to "perfect" self-organization in monolayers, as found for spacer-containing polymeric lipids,^{12,13} or for so-called "hairy-rods".¹⁹ Polymers with a less suited structure may either give less perfect monolayers or not spread at all, despite a notable amphiphilicity.¹

Whereas the molecular structure of the copolymer series **1–9** provides good to excellent thermal properties,⁹ it was not clear whether it would still allow efficient self-organization. The copolymers do not fit into the category of either "polymeric lipids" or "hairy-rods", as they lack a highly rigid backbone as well as classical amphiphilic side groups with hydrophilic groups and long hydrophobic chains. Though polar and hydrophobic fragments are still present, these fragments are reduced to a minimum, and their partition within the macromolecules does not always allow clear separation of the hydrophilic and hydrophobic regions (cf. Figure 1).

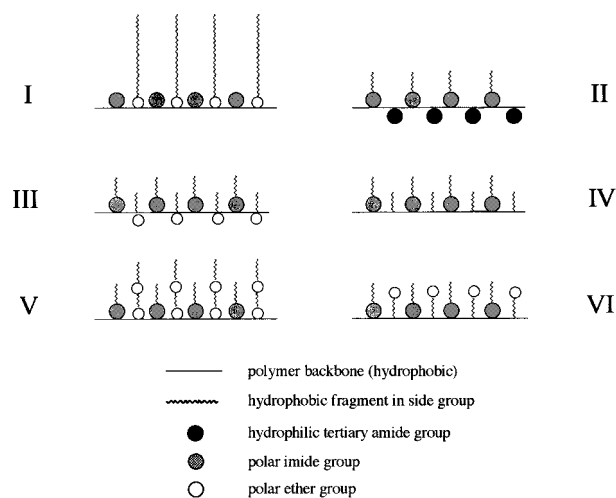


Figure 1. Models of the copolymers' amphiphilic structure.

Materials and Methods

All solvents used were analytical grade. Water was purified by a Milli-Q system. The synthesis of the copolymers, their characterization, and their thermal properties in bulk have been described previously.⁹

Monolayer experiments and LB deposition were performed on a pure aqueous subphase. Two commercial film balances were used which allow monolayer transfer (Lauda 2 with a Langmuir pressure pick-up system and Meyer Feintechnik "Fromherz type",²⁰ with a Wilhelmy pressure pick-up system), as were two home-made ones (with a Wilhelmy pressure pick-up system).^{21,22} In addition, a home-made film balance which enables symmetric compression by two movable barriers was employed (Wilhelmy pressure pick-up system).²³ If not stated otherwise, amphiphiles were spread either from chloroform solutions (concentration about 0.5 mg/mL) or in the case of copolymers **7a–d** from THF/CHCl₃ mixtures (1/9 v/v). Surface pressure–surface potential (Π – ΔV) isotherms are studied using the vibrational plate method.²² Brewster angle micrographs were taken with a model BAM1 (Nanofilm Technology). Monolayers were transferred at 25 °C with a deposition speed of 7 mm/min using the film balance Lauda 2.

Viscometry was performed with a semiautomatic Ubbelohde capillary viscometer (Schott). UV/vis spectroscopy (SLM Aminco DW-2000) was done on samples on quartz supports. For time of flight secondary ion mass spectroscopy (ToF-SIMS;²⁴ Charles Evans & Associates), a 5 kHz pulsed Ga⁺ primary beam (15 kV, 530 pA) was used. The total ion fluence for one set of images was kept below 3×10^{12} ions/cm², ensuring static conditions. The studies were performed on silicon wafers which were hydrophobized with hexamethyldisilazane. Hydrophobized silicon wafers were used as well for atomic force microscopy (AFM; Autoprobe CP, Park Scientific Instruments; contact mode in air, with Ultralever silicon tips). X-ray studies were performed with a powder diffractometer model D-500 (Siemens), using Ni-filtered Cu-K_α irradiation ($\lambda = 0.154$ nm).

Results and Discussion

Spreading Behavior. Except for octadecyl vinyl ether, the diverse parent monomers do not form monolayers at the air–water interface; neither do the maleimides nor the vinyl ethers nor the styrenes. Considering the lack of long hydrophobic chains and assuming a small solubility in water, this is not surprising.

The different structures of amphiphilic copolymers studied vary the relative importance of the polar/hydro-

(14) Green, J. P.; Phillips, M. C.; Shipley, G. G. *Biochim. Biophys. Acta* **1973**, *330*, 243.

(15) Vierheller, T. R.; Foster, M. D.; Schmidt, A.; Mathauer, K.; Knoll, W.; Wegner, G.; Satija, S.; Majkrzak, C. F. *Macromolecules* **1989**, *22*, 3475.

(16) Mathauer, K.; Schmidt, A.; Knoll, W.; Wegner, G. *Macromolecules* **1995**, *28*, 1214.

(17) Teerenstra, M. N.; Vorenkamp, E. J.; Schouten, A. J.; Nolte, R. J. M. *Thin Solid Films* **1991**, *196*, 153.

(18) Cochlin, D.; Laschewsky, A. *Eur. Polym. J.* **1994**, *30*, 891.

(19) Wegner, G. *Ber. Bunsen-Ges. Phys. Chem.* **1991**, *95*, 1326.

(20) Fromherz, P. *Rev. Sci. Instrum.* **1975**, *46*, 1380.

(21) Albrecht, O. *Thin Solid Films* **1983**, *99*, 227.

(22) Vogel, V.; Möbius, D. *J. Colloid Interface Sci.* **1988**, *126*, 408.

(23) Dörr, A. Entwicklung, Konstruktion und Aufbau einer Filmwaage zur Untersuchung monomolekularer Schichten. Master thesis, FH Wiesbaden, Germany, 1993.

(24) Schueler, B. W. *Microsc. Microanal. Microstruct.* **1992**, *3*, 119.

philic and hydrophobic fragments and the partition of these fragments within the copolymers, as outlined schematically in Figure 1. The different structures comprise one "classical" amphiphilic polymer with long hydrophobic chains and a clear-cut separation of the polar and hydrophobic parts (type I, **11f**), as well as structures with strongly reduced hydrophobic tails (types II (series **10**), III (series **9**), and IV (series **7**), the content of polar groups decreasing from types II to IV). Also, some copolymers have structures in which the polar/hydrophilic and hydrophobic fragments are no longer separated clearly but are increasingly intermingled as in types V (series **1–6**) and VI (series **8**).

In contrast to the monomers, all the copolymers studied, i.e. also those of unconventional amphiphilic structure, form stable monolayers at the air–water interface. The copolymers, in particular the ones of series **7–9** with styrenes, give very viscous, "rigid" monolayer films. Hysteresis experiments demonstrated the reversibility of the isotherms at surface pressures below 10 mN/m. Further compression however, above the kinks in the isotherms which are assumed to be the collapse points, leads to irreversible curves.

If not stated otherwise, the discussion of the curves refers to results obtained with a rectangular trough equipped with a Wilhelmy pressure pick-up system by one-sided compression. However note that, for the copolymers studied, the absolute values recorded for the surface pressure of the monolayers depend strongly on the film balance used. If the monolayer is compressed by one movable barrier only ("one-sided compression"), film balances equipped with a Langmuir pressure pick-up system gave systematically much higher collapse pressures than systems equipped with a Wilhelmy plate (about a factor of 2–3). However, if the monolayer is symmetrically compressed by two movable barriers ("two-sided compression"), results correspond to ones obtained with a Langmuir system. The trough geometry influenced the results, too. Isotherms were poorly reproducible with a circular trough,²⁰ depending sensitively on the absolute amount of copolymer spread. We attribute this to the rigidity of the copolymer films. In particular when a Wilhelmy pressure pick-up system with one-sided compression is employed, a lateral displacement of the filter paper plates by the compressed film is observed which leads to low apparent film pressures.

The isotherms exhibit only a very weak temperature dependence between 20 and 40 °C, as reported for other maleimide-based copolymers previously.^{10,11} The curves expand slightly whereas collapse pressures are marginally reduced. The following presentation and discussion are therefore confined to isotherms at 20 °C.

Copolymer **11f** served as a reference, as it has a "classical" amphiphilic structure with long hydrocarbon chains and the polar groups well placed at one side of the macromolecule (Figure 1, type I). Not surprisingly, the isotherm shows a "normal", rather featureless form for an amphiphilic polymer (Figure 2), with high collapse pressure and fairly large collapse area, which compares well with the isotherms of related "conventional" amphiphilic maleimide copolymers.^{10,11} The backbone is obviously sufficiently polar to enable monolayer formation and does not interfere with the spreading. The large collapse area of ca. 0.32 nm²/repeat unit for one alkyl chain may point to some steric crowding of the polymer backbone disturbing the packing of the octadecyl chains, as three out of four carbons are substituted and flexible spacer groups are missing.^{12,13} Though such maleimide copolymers with classical amphiphilic structure do not appear as systems of choice if the most perfect self-organization

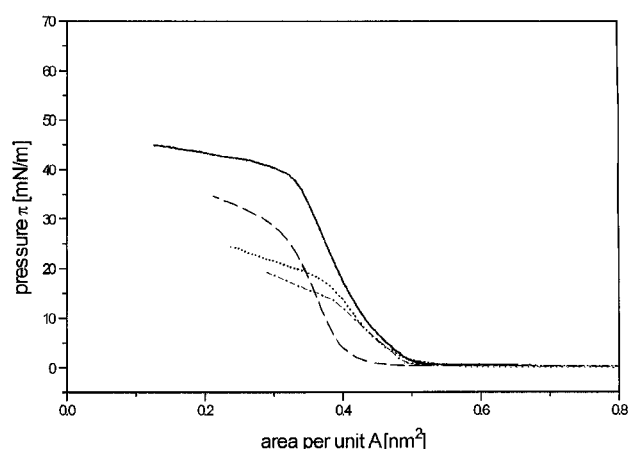


Figure 2. Surface pressure–area (Π – A) diagrams at 20 °C: (· · ·) **5a**; (– – –) **5e**; (– · –) **10a**; (—) **11f** (one-sided compression, Wilhelmy pressure pick-up system).

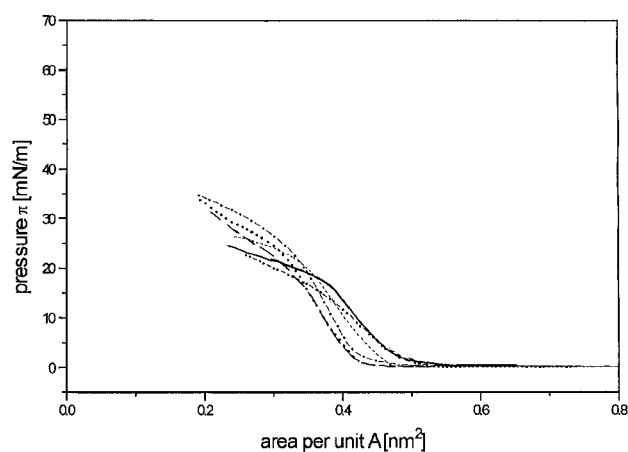


Figure 3. Surface pressure–area (Π – A) diagrams at 20 °C: (– – –) **1c**; (– · –) **2c**; (· · ·) **3c**; (– · –) **6c**; (—) **9c**; (– · –) **10c** (one-sided compression, Wilhelmy pressure pick-up system).

is looked for, the results demonstrate their basic usefulness for Langmuir monolayers.

In the copolymer series **1–10**, the long alkyl chains present in ref **11f** are replaced by benzene rings to produce "condensed" amphiphilic structures (Figure 1, types II–VI). Series **10** is structurally closest to the conventional type I, disposing of strongly hydrophilic moieties by means of the pyrrolidone rings, which may be considered as a hydrophilic "main chain spacer",^{13,25,26} but lacking long aliphatic chains (type II). With a similar amphiphilic structure to alternating copolymers of styrene and maleic acid,²⁶ copolymer series **10** is characterized by a much higher hydrophilic–hydrophobic balance than series **1–9** and by a certain flexibility of the backbone. Copolymers **10** spread easily into monolayers whose isotherms exhibit the rounded shape which is frequently observed for polymers, as exemplified for **10a** and **10c** (Figures 2 and 3). The collapse areas of about 0.4 nm²/repeat unit correspond roughly to ref **11f**, but the collapse pressures of about 18 mN/m are much lower than that for **11f**. Note that this is also true if a Langmuir pressure pick-up system is used, for which collapse pressures of about 40 mN/m are measured for series **10**. The reduced collapse pressures can be explained by only the small hydrophobic residue being present. Within the series, different substituents on the *N*-phenylmaleimide modify the isotherms

(25) Schneider, J.; Erdelen, C.; Ringsdorf, H.; Rabolt, J. F. *Macromolecules* **1989**, *22*, 3475.

(26) Hodge, P.; Koshdel, E.; Tredgold, R. H.; Vickers, A. J.; Winter, C. S. *Br. Polym. J.* **1985**, *17*, 368.

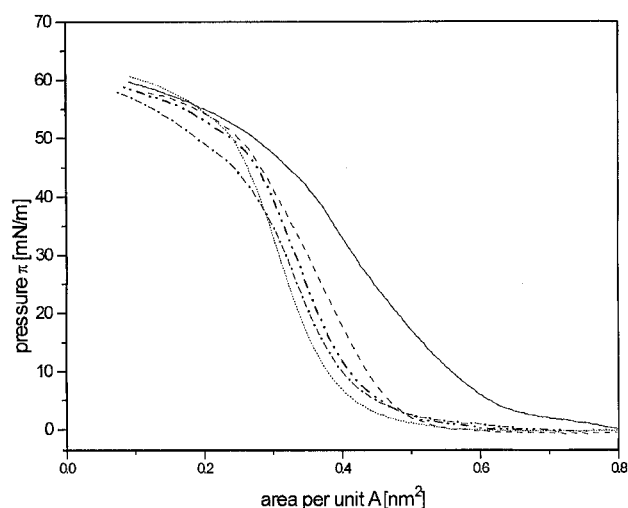


Figure 4. Surface pressure–area (Π – A) diagrams at 20 °C: (···) **8a**; (—) **8b**; (---) **8c**; (-·-·) **8d**; (- - -) **8c** (two-sided compression, Wilhelmy pressure pick-up system)

only slightly (compare **10a** and **10c** in Figures 2 and 3), only **10b**, with two bulky CF_3 substituents on the ring, exhibiting a slightly larger collapse area (cf. series **8** in Figure 4).

Throughout the copolymer series **1–9**, the structure of the compact, hydrophobic maleimide substituents is rather uniform from the amphiphilic point of view. In contrast, the amphiphilic structure of the substituents deriving from the electron-rich comonomer differs notably for the various series, thus resulting in amphiphiles of types III and VI (Figure 1). Nevertheless, the various series show a surprisingly similar spreading behavior, giving “stiff” films with rather low collapse areas in the range between 0.3 and 0.4 $\text{nm}^2/\text{repeat unit}$ (Figure 3). The collapse areas of series **7–9** made from styrenes are slightly larger than those of series **1–6** made from vinyl ethers. The collapse pressures are apparently low with about 15–25 mN/m when recorded by a Wilhelmy system upon compression by one movable barrier only (“one-sided compression”) (Figure 3). The curves appear more “smeared”, and the collapse pressures are in general somewhat lower for the copolymer series **7–9** made with styrenes than for the copolymer series **1–6** made with vinyl ethers. However, collapse pressures appear to be very high with 50–70 mN/m when recorded by a Langmuir system or by a Wilhelmy system upon two-sided compression (see Figures 4 and 5), as discussed above. This discrepancy is attributed to the extreme rigidity of the copolymer films, compared to more “classical” amphiphilic polymers. The differences of the collapse pressures within the series seen by the Wilhelmy system upon one-sided compression are therefore not necessarily indicative of different stabilities of the polymer monolayers but seem rather to reflect the increasing rigidity of the films.

Within a given copolymer series, the differences are small for different maleimide comonomers, as exemplified for series **8** in Figure 4. Copolymers **8a** and **8c–e** give similar isotherms. Only copolymer **8b**, which bears two trifluoromethyl substituents, exhibits significantly higher areas per repeat unit. This is also true in the series **2**, **7**, **9**, and **10**, where the comparison can be made that members **a**, **c**, **d**, and eventually **e** pack comparably, whereas members **b** made with *N*-[3,5-bis(trifluoromethyl)phenyl]maleimide require somewhat larger areas. This can be understood by the increased number of ring substituents. A prominent exception is only found for series **5** (Figure 2). Here, the isotherm of **5a**, which bears two pentafluorophenyl groups, exhibits the very low collapse

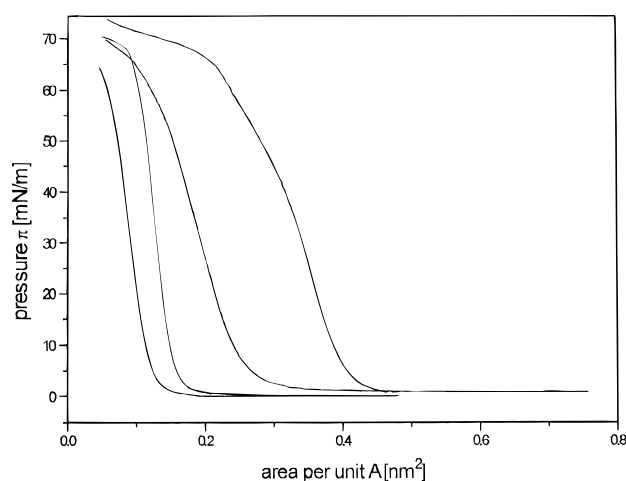


Figure 5. Surface pressure–area (Π – A) diagrams of **2a** at 20 °C, spread from CHCl_3/THF mixtures. From left to right: volume fraction of THF = 0.5, 0.2, 0.1, and 0 (Langmuir pressure pick-up system).

pressure of 14 mN/m and a higher compressibility compared to that of **5e**, which bears only one pentafluorophenyl group and behaves much like the other vinyl ether copolymers (cf. Figure 3).

The spreading experiments show that all copolymers form stable monolayers, despite their unusual structure and, in particular, despite the absence of long hydrophobic chains and the predominance of aromatic groups. Also, the absence of particular hydrophilic groups does not pose problems. This is true for all of the strongly varying amphiphilic structures (Figure 1) and all the hydrophilic–hydrophobic balances realized. Also, this is independent of the extent of fluorination. The high density of substituents on the polymer backbone and the lack of spacer groups do not present prohibiting obstacles. The collapse pressures are surprisingly high. But the general shape of the isotherms is more “smeared”, and the collapse points appear less clear than those for polymers with a classical amphiphilic structure such as **11f**. This is particularly true for the copolymer series **7–9** made with styrenes. Considering that the copolymers of series **1–9** bear two aromatic residues per repeat unit, the areas occupied per hydrophobic residue are substantially smaller than those for the more conventional polymer series **10** and **11f** (Figure 2), pointing to nonideal spreading of the copolymers: the extension of the polymer coils in two dimensions seems to be limited. We attribute this behavior to the important steric crowding of the polymer backbones due to the high degree of substitution. Three out of four carbons of the repeat unit, or even four out of four in the case of series **9**, bear substituents, rendering an efficient packing of the hydrophobic groups difficult. This may also explain why the copolymers of the different amphiphilic structures III and VI behave nevertheless quite similarly: the crowded backbone predominates the spreading behavior. In contrast for series **10**, the pyrrolidone “main chain spacer” helps spreading and efficient packing, but the hydrophobe content is small, thus explaining the relatively low collapse pressures.

It is worth noting that there is no obvious difference in the pressure–area isotherms when comparing copolymers where both aromatic rings bear mixed hydrocarbon/fluorocarbon substituents with those who bear hydrocarbon substituents only. This differs from the spreading behavior of low molar mass amphiphiles with mixed

aliphatic hydrocarbon and fluorocarbon chains, which was explained by their incompatibility.^{27,28}

Influence of the Spreading Solvent. As efficient decoiling of the random, three-dimensional coils going from bulk solution to the gas–water interface is crucial,¹ we wondered about the influence of the spreading solvent on the monolayers. In fact, there are some reports demonstrating the sensitivity of polymeric monolayers to the choice of solvent.²⁹ Taking two bulky hydrophobic residues per repeat unit into account, the collapse areas of the copolymers are rather low. This could be explained by a lesser order of the monolayer arrangement of the thermostable copolymers than found for classical amphiphilic polymers but could also be due to an incomplete decoiling.

Therefore solvent effects were studied exemplarily for copolymer **2a**, as illustrated in Figure 5. The isotherms discussed here are recorded with a film balance equipped with a Langmuir pressure pick-up system, thus explaining the high collapse pressures.

First of all, the influence of the concentration of the copolymer in the standard solvent, i.e. analytical grade chloroform (99% CHCl₃ stabilized by 1% ethanol), was verified. No effect was observed for concentrations up to 1 g/L.

However, differences can show up when the spreading solvent is modified. The use of benzene and CHCl₃ yields the same spreading curves as do mixtures of CHCl₃ containing 20% by weight of methanol or of F₂CIC–CFCl₂. The consistency suggests that indeed maximal spreading is achieved in these solvents. In contrast, mixtures of CHCl₃ containing THF or acetone, respectively, reduce the apparent collapse areas substantially, e.g. from about 0.3 to 0.1 nm²/repeat unit for 20% by weight of cosolvent present. The apparent collapse areas decrease continuously with increasing content of THF (Figure 5) whereas the general form of the isotherms and the collapse pressures is preserved. Unfortunately, the reasons for these effects are not clear.

A first possible explanation could be the water miscibility of the cosolvents acetone and THF, e.g. transferring/precipitating the polymer partially in the aqueous sub-phase. Such an effect could be seriously enhanced by a preferred evaporation of CHCl₃ (b.p. 61.2 °C). But though the boiling point of THF (65.4 °C) is higher than that of CHCl₃, the boiling point of acetone (56.2 °C) is lower. It might be argued that the ternary azeotrope of CHCl₃, ethanol, and H₂O (92.5%/4%/3.5% v/v/v, b.p. 55.5 °C) must be compared instead of pure CHCl₃, but there would always be much pure CHCl₃ left after the complete evaporation of the azeotrope to assure dissolution of the copolymers. Moreover, the affinity of methanol for water is even higher than that of THF or acetone, and its boiling point (64.7 °C) is higher than that of CHCl₃ too. Nevertheless, no negative effects are seen when methanol is added to the spreading solvent up to 20% by volume. Therefore, the hypothesis seems not to be valid.

An alternative possible explanation could be the quality of the spreading solvent. The better the solvent, the larger the dimensions of the random coil in solution, which should facilitate the conformational rearrangement into a two-dimensional monolayer. A direct measure of the expansion of the polymer coil in solution is the intrinsic viscosity $[\eta]$, which was measured for **2a** in various spreading solvents (Figure 6). It was found that $[\eta]$ decreases in the following solutions in the order chloroform ($[\eta] = 54$ mL/g

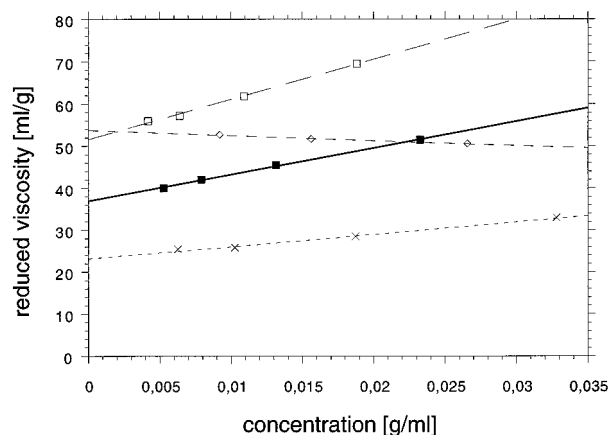


Figure 6. Reduced viscosity of **2a** in various spreading solvents: (■) THF; (□) THF/CHCl₃; (◇) CHCl₃; (×) benzene.

$g) \geq$ chloroform/THF, 4:1 ($[\eta] = 52$ mL/g) > THF ($[\eta] = 37$ mL/g) > benzene ($[\eta] = 23$ mL/g). This means that the best spreading is observed for the solvents with the highest and the lowest values of $[\eta]$, whereas, in the poor spreading solvent CHCl₃/THF, 4:1, $[\eta]$ comes close to the maximal value. In conclusion, the expansion of the polymer coils in the spreading solution is not related to the capability, or incapability, to form well-organized monolayers. The solvent dependence of the spreading of polymers is hence still awaiting clarification.

Surface Potential. An important characteristic of Langmuir films is their surface potentials. The changes of the surface potential of water with the addition of a monolayer ΔV are caused by the superposition of oriented dipoles of the head groups and of the ends of the hydrophobic chains. Due to the strongly differing electronegativities of hydrogen and fluorine, the signs of the dipole moments of the C–H and C–F bonds are opposed. Hydrocarbon terminal groups give a positive contribution to ΔV in monolayers, whereas fluorocarbon terminal groups give a negative one:^{22,30} CH₃ was suggested to contribute +0.66 V, and CF₃, to contribute –0.6 V to the surface potential when packed densely,²² though lower values have been discussed for CH₃ groups too.³⁰ As copolymer series **1–9** have comparable polar groups and polymer backbones, therefore keeping their contribution more or less constant, but have different substitution patterns of hydrocarbon and fluorocarbon groups which are regularly spaced due to the alternating character of the copolymers, surface potential studies were of special interest.

For the different copolymer series, three basic types of ΔV –area diagrams are obtained, as illustrated in Figure 7. Copolymers without fluorine content, such as **1e** or **8e**, exhibit monolayers with positive surface potentials of about +0.3 to +0.5 V (Table 2), whereas negative surface potentials of about –0.4 V are observed if both comonomers bear CF groups, such as for **5a** and **6c**. In monolayers made from copolymers with mixed CF/CH substituents, however, surface potentials are always within the range –0.15 to +0.15 mV and often very close to 0 mV even, independent of the compression (Figure 7, Table 2). This unusual behavior is true for copolymers derived from fluorinated maleimides and hydrocarbon comonomers as well as for copolymers made from hydrocarbon maleimides and fluorinated comonomers. Also, the very low values of ΔV are found independently whether short, flexible spacer groups are present, as in the vinyl ether comono-

(27) Elbert, R.; Folda, T.; Ringsdorf, H. *J. Am. Chem. Soc.* **1984**, *106*, 7687.

(28) Elbert, R. Ph.D. Thesis, Mainz, Germany, 1982.

(29) Collins, S. J.; Mahesh, G. N.; Radhakrishnan, G.; Dhathathreyan, A. *Colloids Surf.* **1995**, *A95*, 293.

(30) Taylor, D. M.; De Oliveira, O. N., Jr.; Morgan, H. *J. Colloid Interface Sci.* **1990**, *139*, 508.

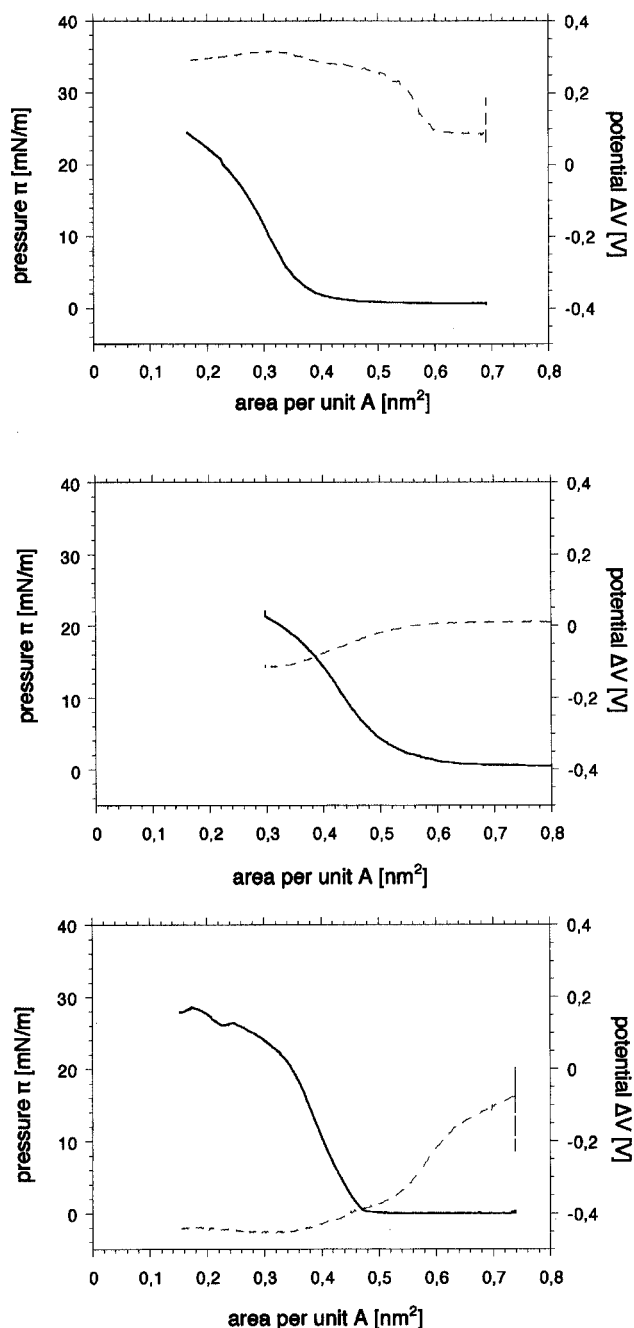


Figure 7. Π - A and ΔV - A diagrams at 20 °C, from top to bottom: **1e**, **9b**, **6c** (one-sided compression).

mers, or are absent, as in the styrene comonomers. In conclusion, the use of CF or CF₃ groups selectively on one of the comonomers, i.e. either on the maleimide or on the electron-rich comonomer, together with structural isomerism (p- vs m-substitution) enables a tuning of the surface potential for given head groups. Of course, appropriate adjustment of the polar groups may result in a similar compensation of the dipole moments, as exemplified by copolymer series **10**.

Though for the copolymers studied it is not trivial that the fluorinated fragments and the hydrocarbon fragments point to the same general direction, the above findings for series **1–9** are best explained by the opposite dipole moments of the CF and CH bonds and by the alternating character of the copolymers. The reversal of the surface potential by exchanging CH by CF groups implies as well that the contribution of the imide group's dipoles to ΔV is small. This suggests an orientation of the imide group preferentially parallel to the water surface. Another

Table 2. Surface Potentials of Monolayers of Maleimide Copolymers at the Surface Pressure 5 mN/m (20 °C, Wilhelmy Pressure Pick-Up System, One-Sided Compression)

R ₃	R ₂	R ₁	ΔV [V]	ΔV [V]	ΔV [V]	ΔV [V]	ΔV [V]
H			$\Delta V = -0.10$ V		$\Delta V = -0.16$ V		$\Delta V = +0.29$ V
		1a		1c		1e	
H				$\Delta V = -0.11$ V	$\Delta V = -0.21$ V		
				2c	2d		
H				$\Delta V = -0.17$ V	$\Delta V = -0.20$ V		
				3c	3d		
H			$\Delta V = -0.41$ V				$\Delta V = -0.10$ V
		5a					5e
H				$\Delta V = -0.41$ V			
				6c			
H			$\Delta V = -0.13$ V	$\Delta V = -0.19$ V	$\Delta V = -0.13$ V	$\Delta V = +0.01$ V	
			7a	7b	7c	7d	
H			$\Delta V = +0.05$ V	$\Delta V = -0.22$ V	$\Delta V = -0.02$ V	$\Delta V = 0.00$ V	
			8a	8b	8c	8d	
OCH ₃			$\Delta V = +0.12$ V	$\Delta V = -0.07$ V	$\Delta V = -0.04$ V	$\Delta V = -0.02$ V	$\Delta V = +0.46$ V
			9a	9b	9c	9d	9e
H			$\Delta V = -0.00$ V	$\Delta V = -0.01$ V	$\Delta V = -0.18$ V		
			10a	10b	10c		

noteworthy comparison is the evolution of ΔV within the different copolymer series. The comparison reveals that the surface potential does not change uniformly with changing substitution on the maleimides, e.g. ΔV evolves differently in the series **7a–d** than in the series **8a–e** or in the series **9a–e** (Table 2). Also comparing positional isomers with respect to the CF₃ substituent, para-substitution leads to more negative surface potentials in the vinyl ether series (compare **2c** and **3c** with **2d** and **3d**) but to less negative potentials in the styrene series (compare **7c**, **8c**, and **9c** with **7d**, **8d**, and **9d**). Accordingly, the arrangement of the copolymers in the monolayer cannot be described by adding fixed increments for each comonomer but depends on the detailed combination of substitution patterns of both comonomers.

Brewster Angle Microscopy. Monolayers of the copolymers were studied by Brewster angle microscopy.^{31,32} Typically for polymers, no interference pattern³³ can be detected for the monolayers; thus, no regular internal structure is found for the films. But the imaging allows us at least to learn the film morphology. Already in the uncompressed state, large flocs are seen (Figure 8). The flocs are merging upon continued compression, but small defects seem to remain. Hence, the monolayers have a structure similar to that of pack-ice. This structure may be responsible for the stiffness of the resulting compressed monolayers as well as for the marked differences in collapse pressures found when using different pressure pick-up systems. Also, drifting flocs can explain the onset of surface potential–area curves at polymer concentrations below the onset of the surface pressure (Figure 7).

Langmuir–Blodgett Films. Though the monolayers of the various copolymers are rather stiff, they could be deposited at surface pressures of 20 mN/m (Langmuir

(31) Hénon, S.; Meunier, J. *Rev. Sci. Instrum.* **1991**, *62*, 936.

(32) Hönig, D.; Möbius, D. *Thin Solid Films* **1992**, *210/211*, 64.

(33) Overbeck, G. A.; Möbius, D. *J. Chem. Phys.* **1993**, *97*, 7999.

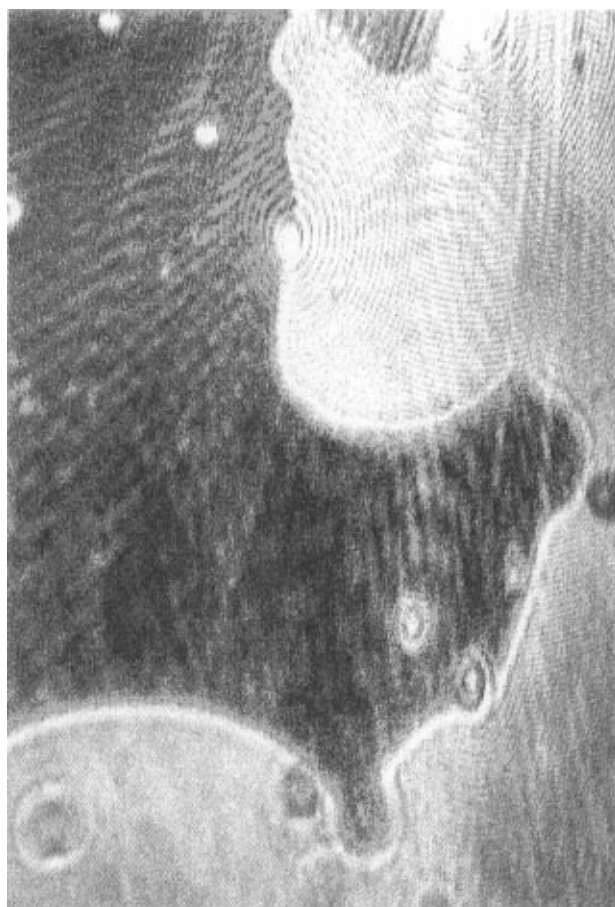


Figure 8. Brewster angle micrograph of a monolayer of **3c** in the uncompressed state, size $100\ \mu\text{m} \times 200\ \mu\text{m}$.

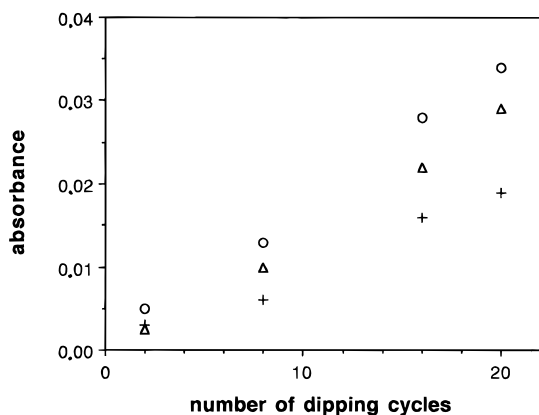


Figure 9. Absorbance of multilayers deposited on quartz ($\lambda = 220\ \text{nm}$); deposition on front side only: (○) **2c**; (△) **7c**; (+) **10c**.

system) on a number of supports, including poly(tetrafluoroethylene) sheets, hydrophobized glass, and quartz slides or silicon wafers. Taking advantage of the aromatic chromophores, the UV measurements of the LB films obtained show a linear dependence of the absorbance on the number of dipping cycles (Figure 9), thus demonstrating reproducible monolayer deposition.

However, the apparent transfer ratios are generally of the order of 0.5 or even lower for copolymers with styrenes. The values are so low because the transfer turned out to be considerably higher on the side facing the compression barrier ("front") than on the opposite side ("back"). This can be shown by carefully washing off the LB film deposited on the back side of the quartz slides with THF. The UV absorbance of the residual multilayer on the front side is only slightly reduced compared to that of the pristine

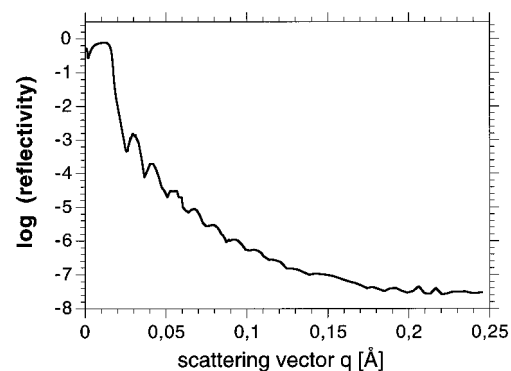


Figure 10. X-ray reflectogram of a LB multilayer of copolymer **3c** (20 layers).

sample. From the relative decrease of the UV absorbance and the knowledge of the overall transfer ratio, separate transfer ratios can be calculated for both the front side and the back side. For copolymers with vinyl ethers and *N*-vinylpyrrolidone, the transfer ratios of the front side are in the range 0.8–0.9, whereas the ratios of the back side are in the range 0.1 only. For copolymers with styrenes, the transfer ratios of the front side are lower with about 0.7, whereas the ratios of the back side are negligibly small (0.05 and less). The decreasing transfer ratios are paralleled by increasing stiffness of the monolayers. Therefore, the difficulties in coating the back side of the supports are attributed to the rigidity of the copolymers, rendering the free flow of the monolayers toward the support difficult.³⁴ This interpretation is supported by the finding that successful deposition takes place when a rectangular trough equipped with a Langmuir pressure pick-up system is used whereas deposition could not be achieved using a circular trough.

X-ray reflectivity studies of the built-up multilayers typically do not reveal Bragg peaks in the diffractograms, but only Kiessig fringes are found, as shown for copolymer **3c** in Figure 10. The overall film thickness of 24 nm divided by the number of transferred layers gives an estimated monolayer thickness of 1.2 nm. The unusual thinness of the polymeric monolayers can be explained by the lack of long hydrophobic chains in the copolymers. This lack is presumably responsible for the missing Bragg peaks too. Either the contrast between the individual layers is not sufficient or the layer structure is less well defined than in conventional LB films. The latter appears more probable, taking the various monolayer experiments and the difficulties in film deposition into account and considering previous work on LB multilayers from maleimide copolymers.¹¹

Analyzing the LB films by time of flight secondary ion mass spectrometry (ToF-SIMS) allows us to judge their quality. As ToF-SIMS is sensitive to the chemical functionalities lying in the topmost layers of the surface, the method enables us to follow gradually the buildup of the multilayer films.

The secondary ion mass spectrum of the naked hydrophobized support shows a strong peak at 73 amu ($\text{Si}(\text{CH}_3)_3^+$), indicating the successful, uniform functionalization of the silicon by hexamethyldisilazane.

In order to verify the regular LB deposition, silicon supports coated with 2, 4, 6, and 8 layers of copolymer **2d** were analyzed on both sides. On the "front" side, the Si^+ fragment intensity (28 amu), related to the silicon substrate, decreases with increasing number of deposited monolayers. It is respectively equal to $48 \pm 4\%$, $23 \pm 3\%$, and $11 \pm 2\%$ of the total spectrum intensity for samples

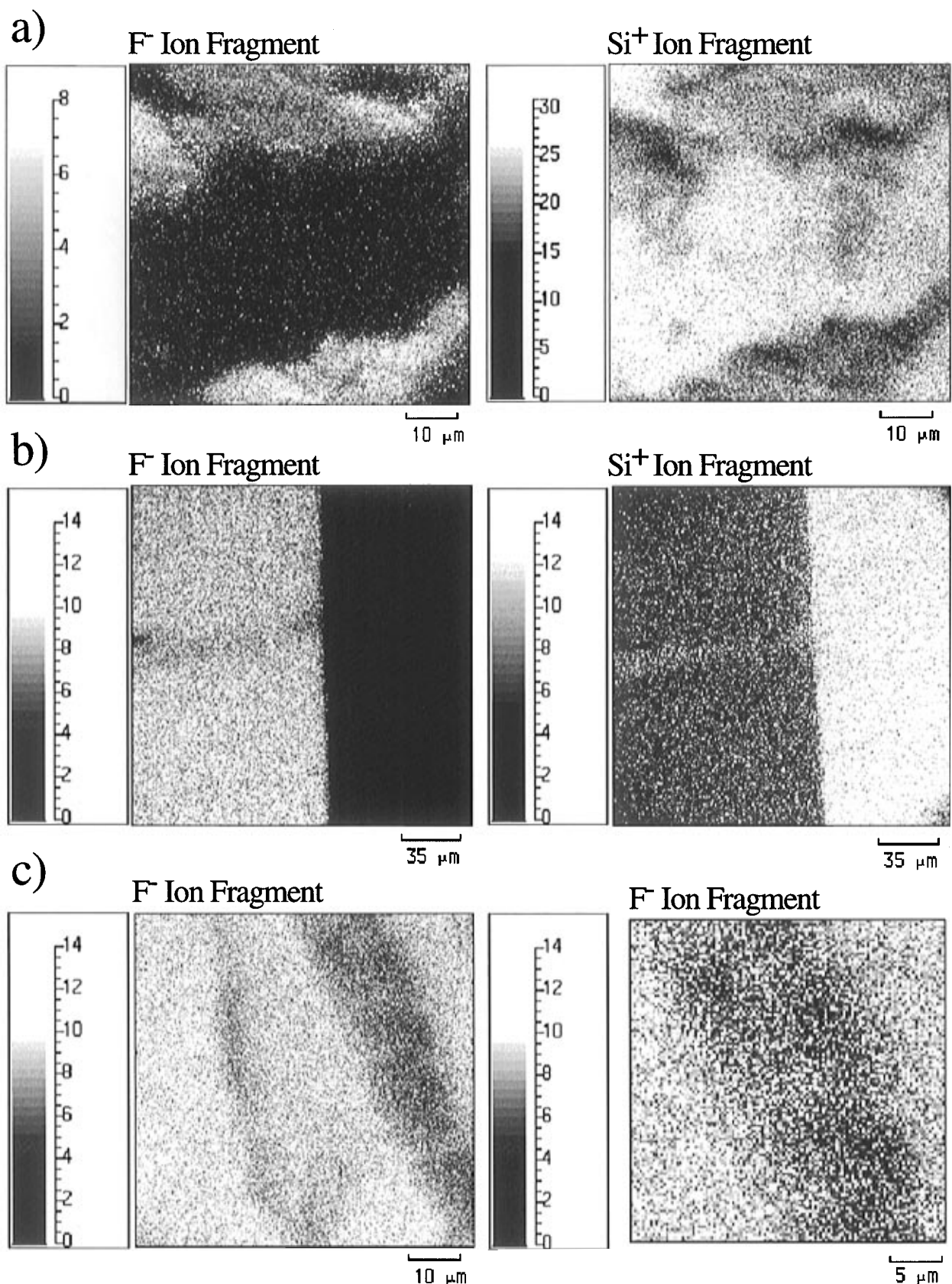


Figure 11. ToF-SIMS mapping of a bilayer of copolymer **2d** on hydrophobized silicon: (a) "back" side; (b) "front" side, edge of a bilayer with a characteristic defect; (c) zoom into a characteristic defect on the "front" side.

with 0, 2, and 4 layers. After the deposition of six layers, signals due to the silicon support became negligible. Assuming a mean emission depth of 10–15 Å for Si⁺ secondary ions,³⁵ this regular decay of the silicon signal with increasing layer number is consistent with a nearly

uniform coverage of the "front" side by each LB layer (cf. Figure 11b).

The simultaneous imaging of characteristic secondary
 (35) Delcorte, A.; Bertrand, P.; Arys, X.; Jonas, A.; Wischerhoff, E.; Mayer B.; Laschewsky, A. *Surf. Sci.* **1996**, *366*, 149.

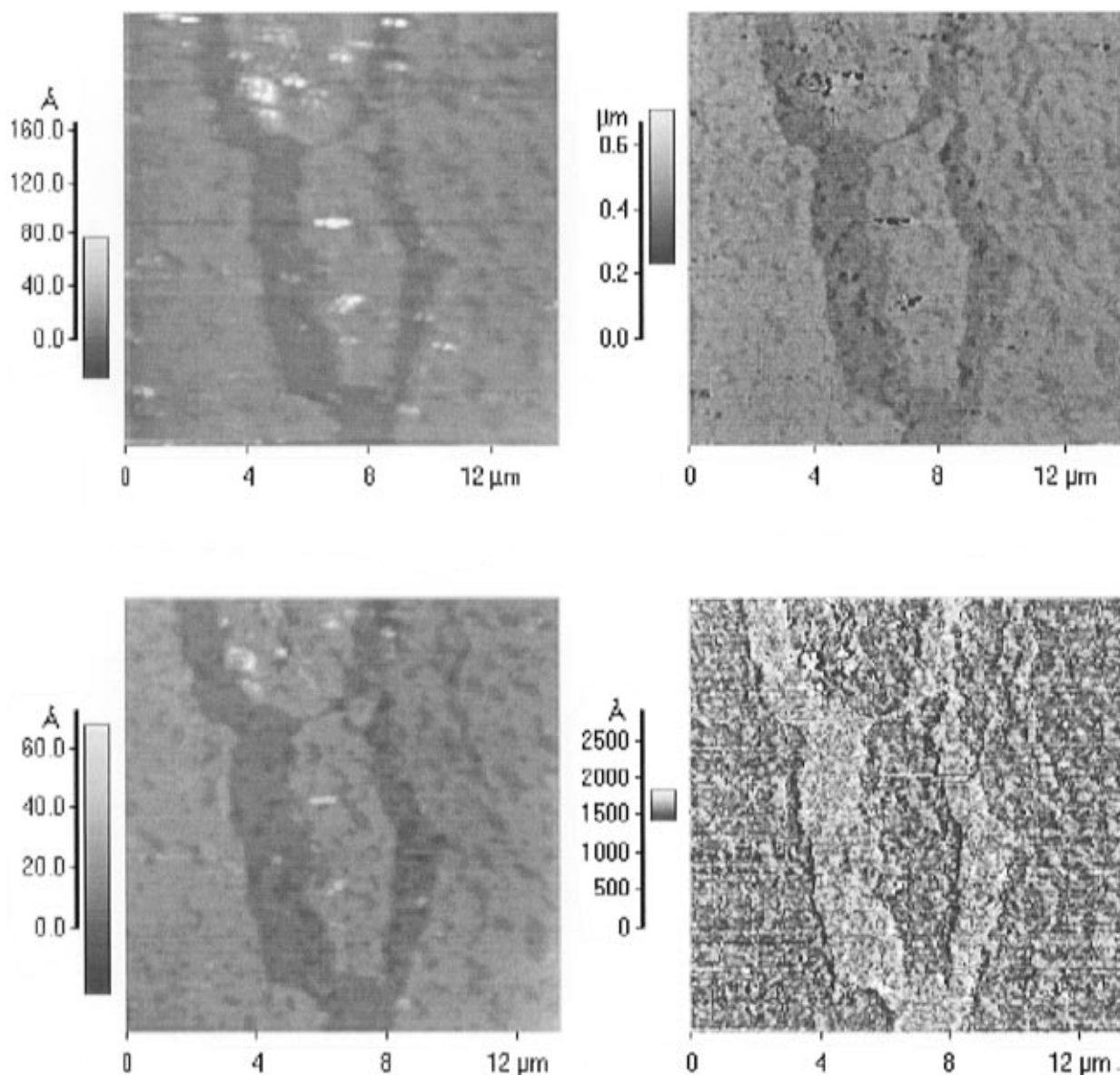


Figure 12. AFM topography (left side) and LFM lateral force scan (right side) of a bilayer of copolymer **2d** on a silicon wafer: top, left to right scan; bottom, right to left scan.

ions of the copolymer (F^-) and of the silicon substrate (Si^+) reveals some interesting features, even with a single polymer bilayer: The complementary fluorine and silicon ion images in Figure 11a confirm that the “back” side of the silicon wafer is poorly covered by the polymer. In contrast, the “front” side exhibits a strong, uniform F^- signal and the border between the bare silicon and the covered zone is sharp and straight (Figure 11b). ToF-SIMS investigations also show the presence of some defects in the “front” side, with the signals of the silicon and of the fluorine fragments being once more complementary as exemplified in Figure 11b and c. Most of the defects are lines of some micrometers in width which separate large, well-covered domains. Zooming into such defects shows that F^- ions are still detected between the coated domains (Figure 11c), thus indicating that some polymeric material is bridging the defects.

Atomic force microscopy (AFM) studies confirm the results obtained by ToF-SIMS, i.e. the formation of coherent coatings with defects present in bilayers. These observations agree well with the images of the spread monolayers seen by Brewster angle microscopy. Topographic images recorded of a bilayer of **2d** (Figure 12) reveal holes, and lateral force microscopy (LFM) images

show that the tip–surface friction force is lower in these holes. Since it is expected that friction will increase with film thickness due to the higher tip indentation and since the friction force of the silicon tip should be much higher on the silicon surface than on the polymer film,³⁶ it can be concluded that the holes correspond to regions covered by a monolayer only. Measuring the height difference between the bilayer and the monolayer allows us to estimate the thickness of the transferred monolayers. A value of about 1.2 nm is found for a monolayer of **2d**, which agrees well with the thickness derived from the X-ray reflectivity studies.

Conclusions

In spite of their rather unusual amphiphilic structure, alternating copolymers of *N*-phenylmaleimides with styrenes and aromatic vinyl ethers are able to self-organize into monolayers at the air–water interface. Though rather stiff, the monolayers can be deposited to give LB multilayers under appropriate conditions. The coatings are probably less well ordered than conventional LB

(36) Meyer, E.; Overney, R.; Brodbeck, D.; Howald, L.; Lüthi, R.; Frommer, J.; Güntherodt, H. *J. Phys. Rev. Lett.* **1992**, *69*, 1777.

multilayers and contain more imperfections. Nevertheless, multilayer buildup is regular, and coherent coatings are obtained. Due to the lack of long hydrophobic chains, the thicknesses of such multilayers are smaller than usual. By virtue of their particular chemical structure, resulting in good thermal stability and high glass transition temperatures,⁹ the copolymers are promising materials for LB multilayers aimed at high-temperature uses. The high stability combined with small thickness and good optical transparency⁹ makes such copolymers as well good candidates for interlayers of alternating non-centrosymmetric LB films for nonlinear optical purposes.³⁷⁻³⁹

Acknowledgment. Technical assistance for measuring surface potentials and taking Brewster angle micro-

graphs was kindly provided by W. Zeiss and D. Spohn. X-ray reflection was kindly measured by A. Jonas. Parts of the work were supported by the EC program "Human Capital and Mobility" (Grant CHRX-CT-0273), by the DG Recherche Scientifique of the French Community of Belgium (convention 94/99-173), by the Fonds National de la Recherche, F.N.R.S. (Crédit aux Chercheurs 1.5.039.95F), and by Hoechst AG.

LA960639+

(37) Hsiung, H.; Rodriguez-Parada, J.; Beckerbauer, R. *Chem. Phys. Lett.* **1991**, *182*, 88.

(38) Hickel, W.; Menges, B.; Althoff, O.; Lupo, D.; Falk, U.; Scheunemann, U. *Thin Solid Films* **1994**, *244*, 966.

(39) Penner, T. L.; Motschmann, H. M.; Armstrong, N. J.; Ezenylimba, M. C.; Williams, D. J. *Nature* **1994**, *367*, 49.